

Evaluation of Models for Earthquake Source Spectra in Eastern North America

by Gail M. Atkinson and David M. Boore

Abstract There have been several relations proposed in the last few years to describe the amplitudes of ground motion in eastern North America (ENA). These relations differ significantly in their assumptions concerning the amplitude and shape of the spectrum of energy radiated from the earthquake source. In this article, we compare ground motions predicted for these source models against the sparse ENA ground-motion database. The source models evaluated include the two-corner models of Boatwright and Choy (1992), Atkinson (1993a), Haddon (1996), and Joyner (1997a,b), and the one-corner model of Brune [as independently implemented by Frankel *et al.* (1996) and by Toro *et al.* (1997)]. The database includes data from ENA mainshocks of $M > 4$ and historical ENA earthquakes of $M > 5.5$, for a total of 110 records from 11 events of $4 \leq M \leq 7.3$, all recorded on rock. We also include 24 available rock records from 4 large earthquakes in other intraplate regions; conclusions are checked to determine whether they are sensitive to the addition of these non-ENA data.

The Atkinson source model, as implemented in the ground-motion relations of Atkinson and Boore (1995), is the only model that provides unbiased ground-motion predictions over the entire period band of interest, from 0.1 to 10 sec. The source models of Frankel *et al.* (1996), Toro *et al.* (1997), and Joyner (1997a,b) all provide unbiased ground-motion estimates in the period range from 0.1 to 0.5 sec but overestimate motions at periods of 1 to 10 sec. The Haddon (1996) source model overpredicts motions at all periods, by factors of 2 to 10. These conclusions do not change significantly if data from non-ENA intraplate regions are excluded, although the tendency of all models toward overprediction of long-period amplitudes becomes more pronounced.

The tendency of most proposed ENA source models to overestimate long-period motions is further confirmed by an evaluation of the relationship between M_s , a measure of the spectrum at 20-sec period, and moment magnitude. A worldwide catalog of shallow continental earthquakes (Triep and Sykes, 1996) is compared to the M_s – M relations implied by each of the source models. The Atkinson source model is consistent with these data, while other proposed ENA models overpredict the average M_s for a given M .

The implications of MMI data from historical earthquakes are also addressed, by exploiting the correlation between felt area and high-frequency source spectral level. High-frequency spectral amplitudes, as specified by the Atkinson and Boore (1995), Frankel *et al.* (1996), Toro *et al.* (1997), and Joyner (1997a,b) source models, equal or exceed the levels inferred from the felt areas of most of the large ENA events, with the notable exception of the Saguenay earthquake. By contrast, high-frequency spectral amplitudes specified by the Haddon (1996) source model agree with the felt area of the Saguenay earthquake but overpredict the felt areas of nearly all other large events. In general, models that fit the Saguenay data—be it intensity data, strong-ground-motion data, regional seismographic data, or teleseismic data—will not fit the data from the remaining earthquakes.

A source model derived from the California database, suitably modified for regional differences in crustal properties, is also evaluated. This model is not signifi-

cantly different from the Atkinson model for ENA. There is an important practical application of this similarity, which we develop as an engineering tool: Empirical ground-motion relations for California may be modified to predict ENA ground motions from future large earthquakes.

Introduction

The prediction of ground-motion amplitudes for future earthquakes, as a function of magnitude and distance, is an important problem in earthquake engineering. It has been established that ground-motion amplitudes at distances ranging from several kilometers to several hundreds of kilometers can be estimated accurately on average, if the underlying earthquake source spectrum is known. Ground motions can be modeled, with comparable accuracy, using stochastic modeling techniques, ray theory, or some combination of the two; examples for eastern North America (ENA) are provided by Ou and Herrmann (1990), EPRI (1993), Atkinson and Somerville (1994), Atkinson and Boore (1995, 1997), and Toro *et al.* (1997). The techniques differ in the way in which the propagation of motions through the Earth's crust is modeled, but all will predict similar motions for the ENA crustal structure, given the same source description. Thus, the accurate specification of the earthquake source spectrum for future earthquakes is a critical issue for the development of reliable ground-motion relations for ENA. It is also the most controversial issue at present. Alternative ENA ground-motion relations are similar to each other in their assumptions regarding the attenuation of ground-motion amplitudes with distance but differ greatly in the assumed near-source amplitude levels and their frequency dependence, for a given moment magnitude.

The reason that the development of ground-motion relations in ENA has remained controversial is that strong-ground-motion data are too sparse to allow ground-motion relations to be derived directly from empirical data, necessitating considerable reliance on models of ground-motion processes. This is an important distinction between ENA and California. In California, strictly empirical approaches are routinely employed to develop ground-motion relations for engineering applications [see Abrahamson and Shedlock (1997) and references therein]. Questions concerning the underlying shape of the source spectrum and its scaling with earthquake magnitude thus have limited consequences for earthquake engineering, in the California case. For ENA, by contrast, these issues have significant engineering implications.

The general approach to the ENA ground-motion problem, given the lack of strong-motion data, is summarized as follows:

“Because of the lack of high-quality data for large earthquakes in ENA, reliable estimates of strong ground motions for future large earthquakes in the region must

necessarily be based either on empirical *S*-wave data from large earthquakes in other, analogous regions or on theoretical extrapolations, based on reliable interpretation of empirical data from small and moderate earthquakes that have previously occurred in the region” (Haddon, 1996).

Recent ENA ground-motion studies have applied one or both of these general approaches to ENA ground-motion modeling, with results differing most significantly with respect to the source spectrum (e.g., Boore and Atkinson, 1987; Toro and McGuire, 1987; Boatwright and Choy, 1992; EPRI, 1993; Atkinson and Boore, 1995, 1997; Frankel *et al.*, 1996; Haddon, 1996; Toro *et al.*, 1997; Joyner, 1997a,b).

In this article, we critically examine the implications, for ground-motion prediction, of the following proposed source spectral models for ENA:

- the single-corner-frequency Brune (1970, 1971) model, as independently implemented in the ENA ground-motion relations by Frankel *et al.* (1996) and by Toro *et al.* (1997; originally published as EPRI, 1993);
- the empirical model of Boatwright and Choy (1992), as determined from analysis of teleseismic signals of intraplate earthquakes;
- the empirical model of Atkinson (1993a), as implemented in the ENA ground-motion relations of Atkinson and Boore (1995, 1997);
- the theoretical model of Haddon (1996); and
- the empirical model of Joyner (1997a,b).

For comparison purposes, we also evaluate the applicability of an empirical model derived from the larger California database (Atkinson and Silva, 1997), with appropriate modifications for regional crustal differences. Finally, we discuss the source model implied for ENA by the SSHAC (1996) process; the underlying source spectrum is not directly specified for this model but can be inferred from the ground-motion amplitudes.

Each of the source models is evaluated by using it to make ground-motion predictions for ENA, which are then compared to the ENA ground-motion database; comparisons are made for all magnitude–distance combinations for which there are observations. The goal is to determine whether the sparse ENA ground-motion database is sufficient to discriminate among the proposed source models. To simplify the comparisons, all predictions and observations are for hard-

rock sites; this is the most prevalent site condition for the database.

ENA Ground-Motion Database

The ground-motion database for moderate-to-large ENA earthquakes includes digital recordings from six mainshocks, and one foreshock, of moment magnitude (M) 4.0 and larger. Aftershock data are not included because they appear to be characterized by lower high-frequency ground-motion amplitudes, for a given moment, than are mainshocks (Boore and Atkinson, 1989; Atkinson, 1993a). There are also about a dozen digitized records from historical ENA earthquakes (Atkinson and Chen, 1997). Finally, there are strong-motion data from four large events from other stable continental interiors that might be considered analogs for large ENA events (subsequently discussed). All seismographic and strong-motion data used in this study were recorded at hard-rock sites. Table 1 lists the instrumental data, and Figure 1 plots the magnitude–distance distribution.

In addition, there are Modified Mercalli intensity (MMI) data from several large historical events. Table 2 lists the MMI data and provides key letters for the events that also have instrumental data, to aid in identifying them on the data plots.

Modern Ground-Motion Data

The modern ENA ground-motion database, extracted from Atkinson and Boore (1995), is comprised of data recorded on rock sites within southeastern Canada and the northeastern United States, with a notable exception. The exception is the M 6.8 Nahanni earthquake of 1985, which occurred in the Northwest Territories, near the western edge of the Canadian shield (also recorded on hard rock). An analysis of the Nahanni earthquakes by the Geological Survey of Canada (Wetmiller *et al.*, 1988) concluded that “The thrust mechanisms, regional stress regime, shallow focal depth, and high-velocity sedimentary rocks in the focal region suggest that the Nahanni earthquakes and particularly the near-field strong ground-motion recorded for the second event are ideal engineering design data for critical facilities in eastern North America.” Thus, although the Nahanni data do not fall strictly within ENA, they fall within the category of “empirical S -wave data from large earthquakes in other, analogous regions” as stated earlier. We have, to date, consistently included the Nahanni earthquake as an ENA event in our ground-motion studies.

Not everyone agrees with our classification of the Nahanni earthquake as an ENA event. It can be argued that if Nahanni is to be included in the ENA database, then we should also include available rock records from other large intraplate earthquakes (A. Johnston, personal comm., 1998). To address this controversy, we have added rock records from the 1976 Gazli, USSR ($M = 6.8$), 1978 Tabas, Iran ($M = 7.4$), and 1991 Georgia, USSR ($M = 6.2$), earthquakes to our database. The advantage of adding these data is that

they improve the magnitude–distance distribution of the database significantly at large magnitudes. The disadvantage is that there is some uncertainty as to whether these events are truly analogous to ENA earthquakes: There may be significant differences, either in the source spectra or in the amplification through the crustal velocity gradient. To accommodate this uncertainty, we will explore the implications of two approaches. One approach is based on the premise that all analogous events should be included; the other excludes all “questionable” (e.g., non-ENA) events. Because the classification of Nahanni as an ENA event is controversial, we group it with the analogous continental earthquakes (e.g., Gazli, Tabas, Georgia, and Nahanni) for the purpose of this exercise.

The ground-motion database, as listed in Table 1, includes digital ground-motion recordings from regional seismographs and digitized strong-motion records. For seismographic stations recording only the vertical component of ground motion, a conversion to a single equivalent horizontal component was made, using the empirical relation determined by Atkinson (1993b) for eastern hard-rock sites. The assumed H/V ratio is near unity at 1 Hz, then increases with frequency to a value of 1.4 for frequencies above 5 Hz. For stations recording horizontal component data, both horizontal components are included.

Historical Instrumental Data

The database includes digitized recordings from several large historical ENA earthquakes, extracted from Atkinson and Chen (1997). The events are the 1925 Charlevoix earthquake of M 6.4, the 1929 Grand Banks earthquake of M 7.3, the 1935 Timiskaming earthquake of M 6.2, and the 1944 Cornwall–Massena earthquake of M 5.8 (moment magnitudes according to Johnston, 1996). It has been demonstrated that the digitized records can recover spectral amplitudes with reasonable reliability (i.e., to within about 20%) in the period range from 0.5 to 20 sec (Atkinson and Chen, 1997). Because a lightly damped single-degree-of-freedom oscillator responds primarily to periods near its natural period, the digitized records can be used to compute response spectra at periods from about 0.5 to 10 sec. These response spectra, for both horizontal- and vertical-component data, are included in Table 1. Vertical-component data are converted to a single horizontal component as described in the previous section; for frequencies less than 1 Hz, the H/V ratio is assumed to be unity.

Intensity Data

The other important body of ground-motion observations for ENA are the MMI data from large historical earthquakes. For most of the damaging ENA earthquakes this century, these data are our only source of information on the levels of high-frequency ground motion (because the digitized historical seismograms cannot recover frequencies above 2 Hz). The relationship between MMI data and spectral source parameters in ENA has been investigated by

Table 1
 ENA Mainshock Data on Hard-Rock Sites

H/V		1.48	1.36	1.22	1.13	1.00	1.00	1.00	
Moment M	hypoR (km)	5% damped PSA (cm/s**2) for Period (sec) =							Event
		0.1	0.2	0.5	1	2	5	10	
6.4	960			1.1E + 01	7.1E + 00	1.7E + 00	3.7E - 01	9.4E - 02	25/03/01 che
6.4	862			5.5E - 01	2.5E - 01	7.9E - 02	2.1E - 02	9.4E - 03	25/03/01 for
7.3	1459				1.3E + 00	4.4E - 01	2.4E - 01		29/11/18 for
7.3	2199				9.6E - 01	2.8E - 01	8.5E - 02		29/11/18 aam
7.3	2199				1.6E + 00	5.5E - 01	1.8E - 01		29/11/18 aam
6.2	616			1.3E + 00	7.4E - 01	4.8E - 01	1.8E - 01	1.4E - 01	35/11/01 aam
6.2	616			3.8E - 01	1.7E - 01	7.7E - 02	5.2E - 02	2.0E - 02	35/11/01 aam
6.2	428				3.4E - 01	5.9E - 02	5.5E - 03	1.8E - 03	35/11/01 buf
6.2	869			2.5E - 01	1.1E - 01	5.2E - 02	1.8E - 02	5.8E - 03	35/11/01 chi
6.2	1430			5.8E - 02	2.8E - 02	2.1E - 02	6.6E - 03	9.3E - 03	35/11/01 csc
6.2	861			1.6E + 00	1.7E + 00	8.5E - 01	2.9E - 01	9.6E - 02	35/11/01 phi
6.2	783			1.1E + 00	1.1E + 00	3.9E - 01	1.8E - 01		35/11/01 wes
6.2	783			1.3E + 00	8.0E - 01	5.1E - 01	3.0E - 01		35/11/01 wes
5.8	389				1.2E + 00	2.6E - 01	3.2E - 02	7.4E - 03	44/09/05 buf
5.8	1007				5.0E - 01	1.3E - 01	3.0E - 02	4.1E - 03	44/09/05 cin
5.8	698				1.3E + 00	2.6E - 01	1.9E - 02	2.4E - 03	44/09/05 geo
5.8	599			2.0E - 01	2.1E - 01	9.1E - 02	2.0E - 02	4.3E - 03	44/09/05 phi
5.8	599			1.6E - 01	1.3E - 01	4.8E - 02	2.6E - 02	6.4E - 03	44/09/05 phi
*6.8	14	1.7E + 03	1.2E + 03	9.3E + 02	6.8E + 02				76/05/17 kara
*6.8	14	1.4E + 03	1.2E + 03	1.0E + 03	4.1E + 02				76/05/17 kara
*7.4	17	6.8E + 02	6.1E + 02	6.9E + 02	2.7E + 02	1.5E + 02	2.6E + 01		78/09/16 dayh
*7.4	17	7.5E + 02	9.6E + 02	4.4E + 02	2.4E + 02	7.3E + 01	2.0E + 01		78/09/16 dayh
*7.4	115	1.6E + 02	2.6E + 02	1.4E + 02	4.1E + 01	1.4E + 01	7.8E + 00	5.1E + 00	78/09/16 ferd
*7.4	115	1.8E + 02	2.4E + 02	1.6E + 02	5.8E + 01	1.6E + 01	1.9E + 01	9.8E + 00	78/09/16 ferd
4.3	275	1.3E + 00	6.8E - 01	1.5E - 01	3.5E - 02				82/01/19 MNT
4.3	324	3.2E - 01	2.7E - 01	1.0E - 01	4.4E - 02				82/01/19 GNT
4.3	389	7.7E - 01	6.0E - 01	2.2E - 01	2.4E - 02				82/01/19 OTT
4.3	537	1.8E - 01	2.1E - 01	9.7E - 02	1.8E - 02				82/01/19 CKO
4.3	724	4.2E - 02	6.8E - 02	4.2E - 02	1.1E - 02				82/01/19 VDQ
4.3	1175	5.8E - 03	9.6E - 03	1.0E - 02	7.0E - 03				82/01/19 MNQ
5.0	143	9.1E + 00	5.0E + 00	1.8E + 00	3.9E - 01				83/10/07 WBO
5.0	180	5.9E + 00	7.2E + 00	1.6E + 00	5.1E - 01				83/10/07 MNT
5.0	199	6.0E + 00	3.5E + 00	2.1E + 00	6.1E - 01				83/10/07 OTT
5.0	246	3.1E + 00	4.0E + 00	2.6E + 00	9.4E - 01				83/10/07 SBQ
5.0	257	4.7E + 00	7.5E + 00	2.5E + 00	5.0E - 01				83/10/07 TRQ
5.0	309	1.1E + 00	1.4E + 00	1.3E + 00	7.9E - 01				83/10/07 GNT
5.0	324	2.1E + 00	2.8E + 00	9.0E - 01	2.2E - 01				83/10/07 GRQ
5.0	339	1.9E + 00	1.5E + 00	1.9E + 00	2.4E - 01				83/10/07 CKO
5.0	501	4.5E - 01	9.3E - 01	6.4E - 01	2.6E - 01				83/10/07 LPQ
5.0	562	3.4E - 01	7.7E - 01	8.8E - 01	2.0E - 01				83/10/07 VDQ
5.0	603	4.0E - 01	6.1E - 01	7.3E - 01	1.8E - 01				83/10/07 GGN
5.0	617	1.8E - 01	2.9E - 01	5.0E - 01	2.4E - 01				83/10/07 EBN
5.0	692	1.8E - 01	2.7E - 01	3.5E - 01	2.0E - 01				83/10/07 KLN
5.0	741	1.5E - 01	3.2E - 01	2.9E - 01	1.2E - 01				83/10/07 HTQ
5.0	776	1.3E - 01	1.9E - 01	2.2E - 01	1.7E - 01				83/10/07 GSQ
5.0	832	1.4E - 01	1.9E - 01	3.7E - 01	2.2E - 01				83/10/07 MNQ
*6.8	8	2.5E + 03	2.8E + 03	7.2E + 02	4.2E + 02	9.0E + 01			85/12/23 S01
*6.8	8	2.7E + 03	2.2E + 03	8.2E + 02	4.8E + 02	1.6E + 02			85/12/23 S01
*6.8	10	5.6E + 02	5.3E + 02	7.6E + 02	2.8E + 02	1.1E + 02			85/12/23 S02
*6.8	10	6.5E + 02	4.1E + 02	6.7E + 02	1.3E + 02	7.8E + 01			85/12/23 S02
*6.8	23	3.1E + 02	1.6E + 02	4.0E + 01	2.3E + 01	1.1E + 01			85/12/23 S03
*6.8	23	2.8E + 02	1.8E + 02	5.8E + 01	3.5E + 01	2.9E + 01			85/12/23 S03
4.5	794	5.2E - 02	8.4E - 02	9.5E - 02	3.0E - 02				86/07/12 EEO
4.5	832	5.8E - 02	1.1E - 01	1.3E - 01	3.4E - 02				86/07/12 CKO
4.5	884	4.7E - 02	4.5E - 02	1.0E - 01	4.6E - 02				86/07/12 OTT
4.5	891	4.1E - 02	5.3E - 02	7.9E - 02	3.0E - 02				86/07/12 WBO
4.5	959	3.2E - 02	5.3E - 02	7.5E - 02	2.7E - 02				86/07/12 GRQ
4.8	21	2.4E + 02	7.7E + 01	1.9E + 01	5.8E + 00				86/01/31 per
4.8	21	2.3E + 02	1.1E + 02	4.1E + 01	9.7E + 00				86/01/31 per
4.8	525	3.7E - 01	7.3E - 01	5.4E - 01	2.9E - 01				86/01/31 SUO
4.8	589	4.9E - 01	7.5E - 01	6.0E - 01	1.8E - 01				86/01/31 EEO

(continued)

Table 1 (continued)

H/V	1.48	1.36	1.22	1.13	1.00	1.00	1.00	Event	
									Moment M
		0.1	0.2	0.5	1	2	5	10	
4.8	603	4.4E - 01	6.3E - 01	3.6E - 01	1.2E - 01				86/01/31 OTT
4.8	741	1.3E - 01	1.7E - 01	1.7E - 01	1.2E - 01				86/01/31 MNT
4.8	776		2.8E - 01	2.7E - 01	1.2E - 01				86/01/31 VDQ
4.8	851	9.1E - 02	1.4E - 01	1.5E - 01	1.3E - 01				86/01/31 SBQ
4.8	871	8.2E - 02	1.4E - 01	1.2E - 01	1.1E - 01				86/01/31 GNT
4.2	100	3.9E + 00	1.9E + 00	2.3E - 01	9.7E - 02				88/11/23 A61
4.2	100	4.2E + 00	1.7E + 00	1.8E - 01	9.5E - 02				88/11/23 A61
4.2	128	3.2E + 00	1.7E + 00	2.1E - 01	1.2E - 01				88/11/23 LPQ
4.2	202	3.7E + 00	1.7E + 00	5.8E - 01	6.3E - 02				88/11/23 DPQ
4.2	232	5.2E - 01	3.3E - 01	1.1E - 01	5.7E - 02				88/11/23 EBN
4.2	315	1.9E - 01	1.5E - 01	1.2E - 01	5.5E - 02				88/11/23 GSQ
4.2	347	6.9E - 01	6.2E - 01	1.3E - 01	2.9E - 02				88/11/23 MNT
4.2	390	6.9E - 01	1.6E + 00	3.2E - 01	3.8E - 02				88/11/23 GRQ
4.2	460	3.8E - 01	5.3E - 01	2.4E - 01	3.9E - 02				88/11/23 OTT
4.2	468	2.8E - 01	3.7E - 01	1.6E - 01	3.1E - 02				88/11/23 WBO
4.2	474	9.1E - 02	9.3E - 02	5.0E - 02	2.9E - 02				88/11/23 GGN
5.8	118	3.3E + 02	1.9E + 02	5.0E + 01	4.5E + 00	1.7E + 00			88/11/25 S01
5.8	118	2.5E + 02	1.7E + 02	3.0E + 01	5.0E + 00	1.8E + 00			88/11/25 S01
5.8	151	1.3E + 02	9.1E + 01	2.0E + 01	1.5E + 01	3.4E + 00			88/11/25 S02
5.8	151	1.1E + 02	1.3E + 02	3.5E + 01	1.8E + 01	2.3E + 00			88/11/25 S02
5.8	112		3.3E + 01	2.1E + 01	3.6E + 00	2.4E + 00			88/11/25 S05
5.8	98	2.5E + 02	2.5E + 02	1.3E + 02	3.1E + 01	6.0E + 00			88/11/25 S08
5.8	98	1.0E + 02	9.7E + 01	3.4E + 01	1.2E + 01	2.5E + 00			88/11/25 S08
5.8	126	7.5E + 01	9.7E + 01	5.0E + 01	2.6E + 01	6.0E + 00			88/11/25 S09
5.8	126	1.3E + 02	1.8E + 02	6.5E + 01	1.8E + 01	3.5E + 00			88/11/25 S09
5.8	118	1.1E + 02	9.4E + 01	2.8E + 01	2.5E + 01	5.3E + 00			88/11/25 S10
5.8	118	1.5E + 02	9.4E + 01	8.8E + 01	2.5E + 01	4.4E + 00			88/11/25 S10
5.8	178	3.1E + 01	5.7E + 01	2.0E + 01	3.3E + 00	1.2E + 00			88/11/25 S14
5.8	178	2.7E + 01	4.1E + 01	1.6E + 01	8.8E + 00	2.4E + 00			88/11/25 S14
5.8	51	1.8E + 02	1.0E + 02	1.8E + 01	5.0E + 00				88/11/25 S16
5.8	51	2.6E + 02	1.4E + 02	4.9E + 01	8.8E + 00				88/11/25 S16
5.8	71	1.5E + 02	1.2E + 02	2.8E + 01	4.1E + 00				88/11/25 S17
5.8	71	1.9E + 02	1.0E + 02	1.4E + 01	3.8E + 00				88/11/25 S17
5.8	96	2.5E + 02	2.2E + 02	6.5E + 01	1.8E + 01	4.4E + 00			88/11/25 S20
5.8	96	1.9E + 02	9.7E + 01	5.7E + 01	1.6E + 01	2.6E + 00			88/11/25 S20
5.8	314	8.2E + 00	1.2E + 01	9.1E + 00	2.9E + 00				88/11/25 GSQ
5.8	333	1.3E + 01	1.6E + 01	6.4E + 00	2.9E + 00				88/11/25 TRQ
5.8	389	4.9E + 00	6.3E + 00	6.5E + 00	1.8E + 00				88/11/25 KLN
5.8	391	8.2E + 00	9.7E + 00	6.6E + 00	1.6E + 00				88/11/25 GRQ
5.8	468	7.8E + 00	8.4E + 00	7.1E + 00	1.3E + 00				88/11/25 WBO
5.8	472	3.7E + 00	7.6E + 00	4.3E + 00	3.3E + 00				88/11/25 GGN
5.8	537	3.8E + 00	4.0E + 00	2.6E + 00	1.4E + 00				88/11/25 CKO
5.8	550	2.0E + 00	1.4E + 00	1.5E + 00	1.3E + 00				88/11/25 LMN
5.8	708	3.8E + 00	3.0E + 00	1.9E + 00	7.0E - 01				88/11/25 JAQ
4.5	27	5.9E + 01	2.7E + 01	2.2E + 00	8.0E - 01				90/10/19 GRQ
4.5	87	1.7E + 01	9.6E + 00	8.5E - 01	1.9E - 01				90/10/19 TRQ
4.5	170	4.7E + 00	2.5E + 00	9.5E - 01	2.2E - 01				90/10/19 WBO
4.5	123	5.5E + 00	4.0E + 00	2.0E + 00	2.7E - 01				90/10/19 OTT
4.5	191	7.6E + 00	2.8E + 00	5.0E - 01	3.9E - 01				90/10/19 MNT
4.5	219	9.5E + 00	6.1E + 00	1.8E + 00	6.2E - 01				90/10/19 DPQ
4.5	407	9.6E - 01	1.6E + 00	4.2E - 01	1.1E - 01				90/10/19 A54
4.5	407	8.9E - 01	1.2E + 00	3.7E - 01	6.1E - 02				90/10/19 A54
4.5	417	3.7E - 01	6.6E - 01	2.1E - 01	1.6E - 01				90/10/19 A11
4.5	417	6.2E - 01	6.8E - 01	3.6E - 01	1.1E - 01				90/10/19 A11
4.5	437	4.2E - 01	7.1E - 01	4.0E - 01	9.2E - 02				90/10/19 A16
4.5	437	5.0E - 01	6.4E - 01	2.7E - 01	8.3E - 02				90/10/19 A16
4.5	437	6.6E - 01	1.0E + 00	3.4E - 01	1.4E - 01				90/10/19 A61
4.5	437	7.1E - 01	6.9E - 01	2.8E - 01	5.5E - 02				90/10/19 A61
4.5	457	4.9E - 01	6.6E - 01	3.1E - 01	7.7E - 02				90/10/19 A64
4.5	457	5.4E - 01	5.7E - 01	2.3E - 01	5.2E - 02				90/10/19 A64
4.5	468	7.7E - 01	1.8E + 00	1.5E + 00	1.0E + 00				90/10/19 A21
*6.2	74	2.0E + 01	3.4E + 01	3.3E + 01	2.1E + 01	9.1E + 00	1.2E + 00		91/06/15 ambr
*6.2	74	2.1E + 01	4.2E + 01	4.8E + 01	2.5E + 01	9.3E + 00	2.8E + 00		91/06/15 ambr

*Indicates a non-ENA intraplate event.

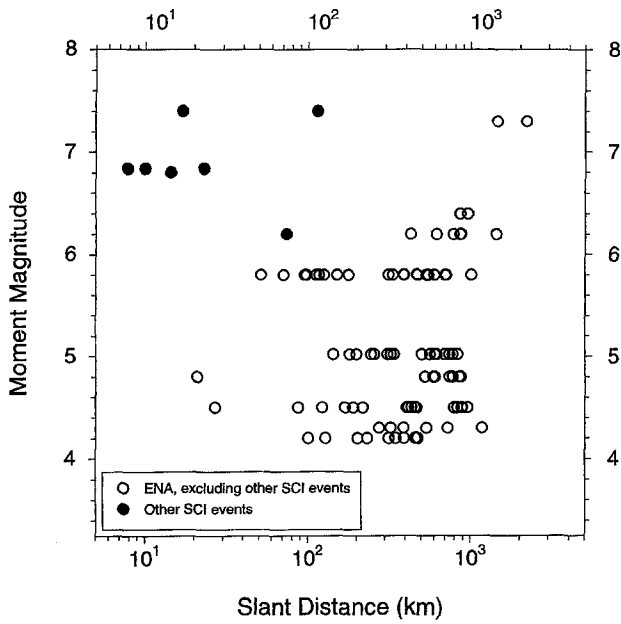


Figure 1. Distribution of ground-motion data (Table 1) for rock sites by magnitude and distance. Open circles show ENA data. Filled circles show data from analogous mid-plate regions.

Table 2
ENA Earthquakes with Ground Motion or MMI Observations

Event	Date	M	Key for PSA Data	Felt Radius (km)
Charlevoix	1925 03-01	6.4	C25	905
Attica	1929 08-12	4.9		340
Grand Banks	1929 11-18	7.2	GB29	1263
Timiskaming	1935 11-01	6.2	T35	825
Ossipee	1940 12-20	5.5		443
Cornwall	1944 09-05	5.7	C44	509
Gazli, USSR	1976 06-17	6.8	G76	
Tabas, Iran	1978 09-16	7.4	T78	
Miramichi	1982 01-09	5.5		404
Gaza (NH)	1982 01-19	4.3	G82	
Goodnow	1983 10-07	5.0	G83	453
Nahanni 1	1985 10-05	6.7		694
Nahanni 2	1985 12-23	6.8	N85	694
Painesville	1986 01-31	4.8	P86	332
Ohio	1986 07-12	4.5	O86	
Saguena y foreshock	1988 11-23	4.2	S88F	
Saguena y	1988 11-25	5.8	S88	1027
Ungava	1989 12-25	5.9		503
Mont Laurier	1990 10-19	4.5	ML90	453
Georgia, USSR	1991 06-15	6.2	G91	

Notes: Events with a PSA key have response spectra data (in Table 1). Felt radii (where listed) are plotted in Figure 6.

Hanks and Johnston (1992), Atkinson (1993a), Bollinger *et al.* (1993), Frankel (1994), Atkinson and Hanks (1995), and Johnston (1996). Based on these studies, we can evaluate at least some of the intensity implications of proposed source spectral models for large events, as described later. The key parameter is the radius of the felt area of the earthquake; these data are given in Table 2.

Source Spectral Models

There have been several models of the source spectrum of acceleration proposed for ENA earthquakes of moderate-to-large magnitudes, as shown in Figure 2. The basis for each of the models is summarized later. These models should be considered as “apparent source spectra” or “effective source spectra,” where *apparent* or *effective* refers to the fact that these representations are what we deduce from far-field observations. They are not physical models of source processes but phenomenological models of the effect that the source processes have on ground motions observed at sites on the Earth’s surface, far removed from the source processes.

To facilitate comparisons of source models, we have expressed them using common functional forms. The general form for the acceleration spectrum at near-source distances is given by

$$A(f) = C(2\pi f)^2 M_0 S(f), \tag{1}$$

where M_0 is seismic moment and $S(f)$ is the displacement source spectrum. The constant C is given by $C = RVFS/$

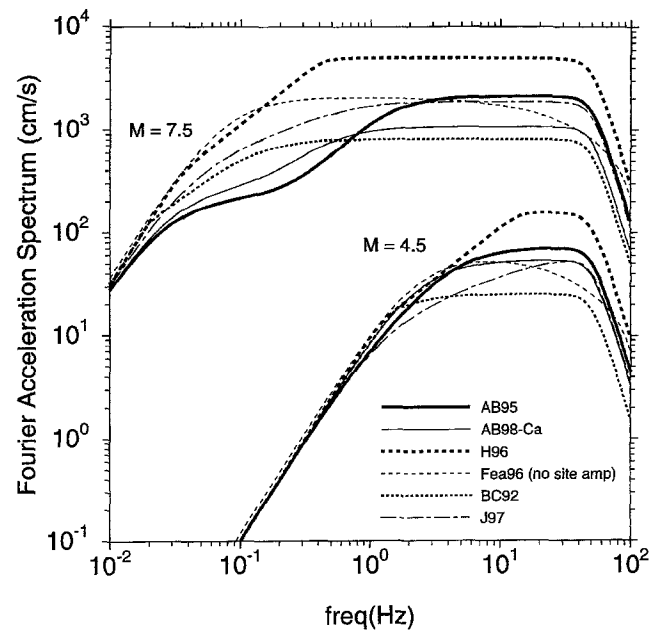


Figure 2. Fourier spectrum of acceleration at $R = 1$ km, according to the source spectral models evaluated in this article. The median of the source models underlying the TAS97 relations is very similar to the Fea96 model; it is not shown because they actually use a range of source model parameters.

$(4\pi R\rho\beta^3)$, where \mathcal{R} is the radiation pattern ($=0.55$ on average for shear waves), V is a partition onto two horizontal components ($=1/\sqrt{2}$), FS is the free-surface amplification ($=2$), R is distance from the source, and ρ and β are the density and shear-wave velocity, respectively, in the vicinity of the source.

The source spectra for each of the models evaluated in this study involve one or two corner frequencies (f_a, f_b) and a relative weighting parameter ε , whose value lies between 0 and 1 (where for $\varepsilon = 1$, the two-corner model is identical to a single-corner Brune model). Table 3 provides the functional form of the spectra, $S(f)$, for each of the models, Table 4 provides the shape parameters (f_a, f_b , and ε), and Table 5

lists the remaining parameters, including physical constants and attenuation and duration models.

All models are implemented for hard-rock sites (near-surface shear-wave velocity > 2.5 km/sec). It is assumed that there is no significant amplification through the ENA crustal profile or due to near-surface rock weathering. Recent seismic refraction experiments for hard-rock sites in eastern Ontario and western Quebec (Beresnev and Atkinson, 1997) have confirmed the appropriateness of this assumption. Typical near-surface shear-wave velocities are >2.5 km/sec; the implied amplification due to the velocity gradient from mid-crustal depths to the surface is negligible (Beresnev and Atkinson, 1997).

We have evaluated the seven source models described in the following.

Boatwright and Choy Model

Boatwright and Choy (1992) (BC92) derived an empirical model for the source spectra of large intraplate earthquakes, based on analysis of teleseismic signals from a global database of such events. It was presented as an ENA source model, using the analogy principle referred to earlier. This model is characterized by two corner frequencies. We

Table 3
Shape of Source Spectra [$S(f) = S_a(f) * S_b(f)$]

Model	S_a	S_b
BC92	$f < f_a : 1$ $f \geq f_a : f_a/f$	$\frac{1}{[1 + (f/f_b)^2]^{1/2}}$
AB95	$\frac{1 - \varepsilon}{1 + (f/f_a)^2} + \frac{\varepsilon}{1 + (f/f_b)^2}$	1
Fea96	$\frac{1}{1 + (f/f_a)^2}$	1
H96	$\frac{1}{[1 + (f/f_a)^8]^{1/8}}$	$\frac{1}{[1 + (f/f_b)^8]^{1/8}}$
AB98-Ca	$\frac{1 - \varepsilon}{1 + (f/f_a)^2} + \frac{\varepsilon}{1 + (f/f_b)^2}$	1
J97	$\frac{1}{[1 + (f/f_a)^2]^{3/4}}$	$\frac{1}{[1 + (f/f_b)^2]^{1/4}}$

Table 4
Corner Frequencies and Moment Ratios

Model	$\log f_a$	$\log f_b$	$\log \varepsilon$
BC92	$M \geq 5.3:\ddagger$ 3.409 - 0.681M	1.495 - 0.319M	—
	$M < 5.3:$ 2.452 - 0.5M	2.452 - 0.5M	—
AB95	$M \geq 4.0:\ddagger$ 2.41 - 0.533M	1.43 - 0.188M	2.52 - 0.637M
	$M < 4.0:$ 2.678 - 0.5M	2.678 - 0.5M	0.0
Fea96*	2.623 - 0.5M	—	—
H96	2.3 - 0.5M	3.4 - 0.5M	—
AB98-Ca	$M \geq 4.8:\ddagger$ 2.181 - 0.496M	1.308 - 0.227M	3.223 - 0.670M
	$M < 4.8:$ 2.617 - 0.5M	2.617 - 0.5M	0.0
J97	2.312 - 0.5M	3.609 - 0.5M	—

*This is the Brune model, for which $\log f_0 = 1.341 + \log [\beta(\Delta\sigma)^{1/3}] - 0.5M$, with $\beta = 3.6$ km/sec and $\Delta\sigma = 150$ bars.

†The specified magnitude corresponds to the point at which $f_a = f_b$.
‡The specified magnitude corresponds to the point at which $\varepsilon = 1.0$.

Table 5
Model Parameters

- $\rho, \beta, V, \mathcal{R}, FS:$
all but Fea96: 2.8, 3.8, 0.71, 0.55, 2.0
Fea96: 2.8, 3.6, 0.71, 0.55, 2.0
- Geometrical spreading (including factors to insure continuity of function):

$$r < 70 \text{ km} : 1/r$$

$$70 \text{ km} \leq r < 130 \text{ km} : 1/70$$

$$130 \text{ km} \leq r : (1/70)(130/r)^{0.5}$$

- $Q:$
all but H96: $680f^{0.36}$
H96: 1350
- Source duration ($a/f_a, b/f_b$):
all but Fea96: $a = 0.5, b = 0.0$
Fea96: $a = 1.0, b = 0.0$
- Path duration:
all but Fea96:

$$r < 10 \text{ km} : 0.0$$

$$10 \text{ km} \leq r < 70 \text{ km} : 0.16 (r - 10)$$

$$70 \text{ km} \leq r < 130 \text{ km} : 9.6 - 0.03 (r - 70)$$

$$130 \text{ km} \leq r : 7.8 + 0.04 (r - 130)$$

Fea96: $\text{all } r : 0.05r$

- Site amplification: 1.0
- Site diminution parameters (f_{\max}, κ)
all but Fea96: 50.0, 0.0
Fea96: 100.0, 0.006

derived relationships for the source spectra, as given in Tables 3 and 4, based on the data presented in Boatwright and Choy's article; these data included tables of M , corner frequencies, and high-frequency spectral levels for a number of intraplate earthquakes. To find the parameters that best matched the spectra presented by Boatwright and Choy, we first converted their P -wave spectral levels to S -wave spectral levels using the relationships discussed in their article (including a corner frequency shift of 1.5 from S to P , for the high corner frequency, and their constant factors accounting for the ratio of P -to- S wave velocities). Least-squares regression was used to fit their high corner frequency as a function of M ; their high-frequency spectral levels were also regressed against M , forcing constant-stress scaling as stipulated in their article. Finally, we solved for their low corner frequency, assuming the functional form for the source spectrum as given in Table 3, and expressed this as a function of M . We verified that the resulting equations provide an accurate description of the spectral levels of the events, as given in Table 3 of their article.

Atkinson and Boore Relations

The ground-motion relations of Atkinson and Boore (1995) (AB95) implement the proposed source model of Atkinson (1993a). This source model, like that of Boatwright and Choy, is an empirical model using two corner frequencies to describe the spectrum. The parameters listed in Tables 3 to 5 are those adopted by Atkinson and Boore (1995). The Atkinson (1993a) model converges with the Brune model, as implemented by EPRI (1993), Toro *et al.* (1997), and Frankel *et al.* (1996), for $M = 4.0$. For larger magnitudes, the Atkinson source spectrum features much lower amplitudes at intermediate-to-low frequencies, relative to those implied by a Brune model.

Frankel *et al.* Relations

The Frankel *et al.* (1996) (Fea96) source model is a single-corner-frequency, ω^2 spectrum with a 150-bar stress parameter [e.g., a Brune (1970, 1971) point source]. The parameter values used in our simulations are those given by Frankel *et al.* (1996, Table A5), except that no site amplification was applied, and the diminution parameter κ was set to 0.006. These two modifications were made in order to simulate motions on hard-rock sites; hard rock is the site condition used in this article, whereas the Frankel *et al.* relations are for a reference site condition of soft rock ($\beta = 760$ m/sec). The parameters used in the simulations are given in Tables 3 to 5.

Haddon Model

The source model of Haddon (1996) (H96) is based on a circular crack model and incorporates postulated average effects of fractional stress drop and directivity. Like the Boatwright and Choy (1992) and Atkinson (1993a) models, the Haddon (1996) model features two corner frequencies. However, the Haddon (1996) model predicts much larger

amplitudes at short-to-intermediate periods, for all magnitudes, than any of the other source models. Haddon (1996) presents his source model in graphical form only. It was thus necessary to fit a function to his model to allow its implementation in the simulations. Working from his Figure 10, we determined that the corner frequencies as given in Table 4, with the functional form given in Table 3, provide an excellent fit to his spectra. [Note: When we overlaid the spectra computed from the derived equations on the spectra in Haddon's Figure 10, we found a uniform offset in amplitudes of 0.05 log units. This offset is due to a rounding error in the relation between seismic moment and moment magnitude. Haddon apparently used

$$\log M_0 = 1.5 M + 16.0$$

rather than the correct relation

$$\log M_0 = 1.5 M + 16.05.$$

The latter equation comes directly from the defining relation of moment magnitude, as given by Hanks and Kanamori (1979): $M \equiv \frac{2}{3} \log M_0 - 10.7$.]

Toro, Abrahamson, and Schneider Relations

The ground-motion relations of Toro *et al.* (1997; originally published as EPRI, 1993) are based on a single-corner-frequency ω^2 source model, similar to that used in the Frankel *et al.* (1996) relations. The Toro *et al.* (TAS97) parameter values are slightly different than those of Frankel *et al.*; Toro *et al.* use a median stress parameter of 120 bars, slightly different crustal constants, and an attenuation function based on modeling of ground-motion propagation in the crustal wave guide. We therefore evaluate the TAS97 model separately from the Fea96 model, based on the ground-motion relations given by Toro *et al.* (1997) in their article. [Note: The source model for the TAS97 relations is not uniquely specified because they vary parameter values to obtain an estimate of uncertainty in ground-motion amplitudes; however, their median source model is very similar to that shown in Figure 2 for Frankel *et al.* (1996).]

Joyner Model

The source model of Joyner (1997a,b) (J97) is an empirical two-corner source model. It was derived by refitting the data of Atkinson (1993a), for the high-frequency spectral level and 1-Hz spectral amplitudes, to a functional form containing two multiplicative terms in f_a and f_b , as opposed to the two additive terms used by Atkinson. The corner frequencies were constrained to follow a self-similar scaling law (e.g., they both scale as moment to the minus one-third power); the slope of the acceleration spectrum between the two corner frequencies is $\omega^{1/2}$.

Modified California Model

We also make ground-motion predictions for ENA using a modified version of the empirical source model developed for California by Atkinson and Silva (1997) (AB98-Ca). This model is included as a test: We wish to determine the extent to which ENA ground-motion observations can be modeled based on conclusions and models drawn from the much larger California empirical database. We do not necessarily expect this model to be applicable to ENA.

In order to place the California source model within the ENA crust, we adjust the empirically inferred California source amplitudes of Atkinson and Silva (1997) to reflect the different crustal properties of generic ENA rock versus generic California rock. The method of adjustment for crustal properties consists of several steps:

1. We begin with the source terms determined by regression of Fourier amplitude spectra of California earthquakes of $4.4 \leq M \leq 7.4$ (from Atkinson and Silva, 1997). The source terms of the regression represent the far-field amplitudes of motion, projected back to a reference distance of 1 km from the fault. They implicitly include the amplification effects of propagation from the source depth through the California crustal velocity structure to the surface, as well as the average effects of kappa, the exponential decay parameter that filters high frequencies in the near-surface sediments (Anderson and Hough, 1984).
2. The amplification factors for a generic California crustal profile are divided out of the California source terms, to remove the effects of the California crustal velocity gradient. The factors for this spectral division are adopted from the California rock amplifications derived by Boore and Joyner (1997).
3. The effect of kappa is removed from the adjusted spectrum of each earthquake (i.e., after division for the crustal amplification effects). The average kappa value implicit in each of the adjusted source terms is determined by fitting a straight line to the log amplitude versus linear frequency (Anderson and Hough, 1984), using only that portion of the spectrum above the corner frequency. Each apparent source spectrum is then divided by the kappa operator of Anderson and Hough (1984), using the determined kappa values. This operation removes the average kappa effects caused by near-surface sediments, so that the adjusted spectra now better represent the source effects. The average kappa values, determined in this step, may be represented by the equation $\text{kappa} = -0.012 + 0.0106 M$.
4. The parameter f_b is determined for each event as the frequency at which one-half of the high-frequency spectral amplitude level is attained (for consistency with the meaning of f_b for the case $\varepsilon = 1$). The values of f_b are regressed against magnitude to obtain the relationship given in Table 4. [The lower corner frequency, f_a , is based on source duration, as given by Atkinson and Silva (1997)].

5. The best-fitting value of ε is then determined for each event, using the prescribed values of f_a and f_b for the given M (i.e., we numerically determine that value of ε for which the average mismatch between the source model equation and the spectral data points are minimized). These values of ε are regressed against magnitude to obtain the relationship given in Table 4.

These model parameters are used with the ENA crustal constants (Table 5) to represent the expected spectral amplitudes from a California source occurring within the ENA crust. [Note: To predict expected spectral amplitudes within the California crust, we would use the same model parameters, but with the appropriate California crustal constants and crustal amplification as specified in Boore and Joyner (1997); the California kappa from Step 3 would also be applied.]

Evaluation of Source Models

It has been demonstrated that the stochastic ground-motion model (Hanks and McGuire, 1981; Boore, 1983) provides accurate ground-motion predictions, on average, if the earthquake source spectrum and regional attenuation are known; in fact, its accuracy is comparable to that of more detailed wave-propagation methods (Atkinson and Somerville, 1994). The accuracy of the specified input parameters is thus the limiting factor for ground-motion prediction, not the stochastic model itself. The stochastic ground-motion model is a well-accepted basis for ground-motion relations, as evidenced by the fact that all published ground-motion relations proposed for ENA within the last 5 or more years have been based on this model (e.g., Boore and Atkinson, 1987; Toro and McGuire, 1987; EPRI, 1993; Atkinson and Boore, 1995; Frankel *et al.*, 1996; Toro *et al.*, 1997). For these reasons, the stochastic model provides a sound basis for a test of the implications of the source models.

We test the applicability of the source spectral models by using each of them, in conjunction with the stochastic model as implemented by the random-vibration computer code of Boore (1996), to make ground-motion predictions for the events listed in Table 1; these predictions are then compared to the observations. The single exception to this procedure is the ground motions for the Toro *et al.* (1997) model. Toro *et al.* give equations for ground motions, based on fitting the amplitudes obtained from many stochastic model simulations (to account for variability in the model parameters). We used their mid-continent equations for moment magnitude (Table 2 in Toro *et al.*, 1997), interpolating their coefficients to provide response spectra at $T = 0.5$ sec (they provide values for the other periods used in our comparisons).

The input parameters required for the stochastic model predictions are the source spectral model, the attenuation model, and a model for the duration of ground motion [e.g.,

see Boore and Atkinson (1987)]. Fortunately, the required attenuation and duration models for the ground-motion predictions are much less uncertain than the source model. This means that the ground-motion comparisons can effectively isolate the effects of source model assumptions.

In general, we adopt the empirical ENA attenuation and duration models used by Atkinson and Boore (1995), which are well supported by data over the distance range from 10 to 1000 km. In this attenuation model, the decay curve for spectral amplitudes in the S window (including S , SmS , Sn , and Lg) has a hinged trilinear form, with amplitudes decaying as R^{-1} for $R \leq 70$ km, as R^0 for $70 < R \leq 130$ km, and as $R^{-0.5}$ for $R > 130$ km; the anelastic attenuation is inversely proportional to Q , where $Q = 680f^{0.36}$. The duration also follows a hinged form. The duration model has two terms:

$$T = T_0 + bR, \quad (2)$$

where the source duration is given by $T_0 = 1/(2f_a)$ (Boatwright and Choy, 1992). The distance-dependent term has slope $b = 0.0$ for $R \leq 10$ km, then $b = 0.16$ for $10 < R \leq 70$ km, $b = -0.03$ for $70 < R \leq 130$ km, and $b = 0.04$ for $R > 130$ km (Atkinson and Boore, 1995).

Exceptions to these assumptions regarding attenuation and duration are made wherever the authors of the proposed source models or ground-motion relations have suggested alternative parameter values. For the Frankel *et al.* (1996) ground-motion relations, the authors have specified the attenuation and duration model (see Table 5), so we have simply used their choices for these parameters. Haddon (1996, 1997) has suggested that $Q = 1350$ for the ENA crust, and thus, we adopt this attenuation for use with the Haddon source model (with the geometric spreading of Atkinson and Boore, 1995). Boatwright (1994) obtained attenuation results consistent with those of Atkinson and Boore (1995), so we apply our attenuation when using the Boatwright and Choy source model. Joyner (1997a,b) uses the Atkinson and Boore (1995) attenuation and duration with his source model, when making ground-motion predictions.

For each proposed source model, we compute the response spectra (5% damped pseudo-acceleration for the random horizontal component of ground motion) for each magnitude and distance for which we have instrumental ground-motion data. The residual corresponding to each data point is calculated as the ratio of the observed ground-motion amplitude (Table 1) to the predicted ground-motion amplitude for the specified model (for the given magnitude and distance). Thus residuals greater than 1.0 imply underprediction of observed values, while residuals less than 1.0 imply overprediction of observed values (e.g., residuals smaller than unity are “conservative” predictions from the engineering viewpoint).

It could be argued that through selection of the constants, attenuation, and duration parameters of the stochastic model, our source-model evaluation could be biased in favor

of one of the models. This is primarily an issue for the Haddon model, because the authors of the other models have either specified these parameters (e.g., Frankel *et al.*) or published studies that support the choices we have adopted (e.g., Boatwright). To be sure that the Haddon model computations are not biased, we examined the computed residuals as a function of distance, for the two best-recorded events (Saguenay and Mont Laurier). We evaluated whether alternative choices for the attenuation model, for both geometric spreading and Q , or an alternative duration model would improve any discernable trends in plots of the residuals versus distance. The factor that makes the largest difference in the residual trends is the selected geometric spreading model. An example of the impact of the selected attenuation is shown in Figure 3, for a period of 0.1 sec. From these evaluations, we concluded that Haddon’s preferred value of $Q = 1350$, with our trilinear geometric spreading, produces the best distribution of residuals versus distance for the Haddon source model. There is very little sensitivity to the duration model, so this is not a significant issue. The average high-frequency residual for the Haddon model, for the Sag-

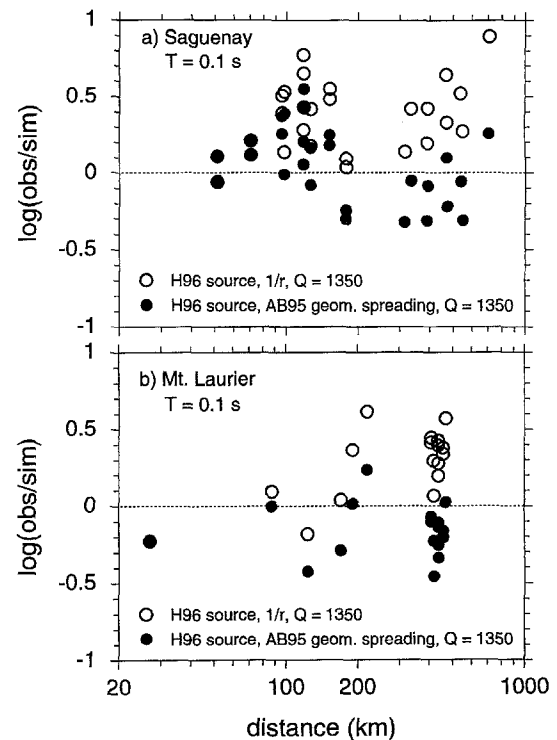


Figure 3. Residuals (log units) of ground-motion predictions made with the Haddon source model, as a function of distance, for the Saguenay (upper) and Mont Laurier (lower) earthquakes, at $T = 0.1$ sec. The effect of alternative assumptions regarding geometric spreading ($1/r$ or trilinear AB95 shape) is shown (open or closed circles, respectively). The effect of alternative assumptions regarding Q or duration are much smaller than the range indicated for the geometric spreading.

uenay and Mont Laurier earthquakes, is near unity. This is expected, because the Haddon source model was derived primarily from study of these two events, and it provides confidence that the average attenuation model selected for use with the Haddon source model is appropriate.

Results of Evaluations

Instrumental Ground-Motion Data

Figure 4 plots, as a function of magnitude, the mean residuals for each of the events of Table 1, for the Boatwright and Choy (1992), Atkinson and Boore (1995), Frankel *et al.* (1996), Haddon (1996), Toro *et al.* (1997), and Joyner (1997a,b) source models, for vibration periods of 0.1, 0.2, 0.5, 1, 2, 5, and 10 sec. The event keys are as given in Table 2. The residuals for the empirical California source model, modified as described previously for ENA crustal conditions, are also shown. Each data point in the figure represents, for the selected period, the average residual for the observations from one earthquake, based on one assumed source model. To avoid clutter, the 95% confidence limits on the mean are shown for only one of the models (AB95). These error bars are of similar length for all models.

If a source model is correct, then the residuals will have an average value near unity and show no discernible trends with magnitude. Deviations from an average event residual of unity are expected for individual events, however, because the interevent component of variability is significant—about a factor of 1.5 (Atkinson, 1995). Thus, a large residual for an individual event is not significant, but the residual becomes significant if it persists over many events.

From Figure 4, it is apparent that some models come much closer to the unity residual target than do others, for particular period ranges. At short periods (0.1 to 0.2 sec), the AB95, Fea96, and J97 models are closest to the target; they underpredict significantly for the Saguenay earthquake (M 5.8) but come close for all other events. Perhaps surprisingly, the modified California model is also close to the target. The BC92 source model significantly underpredicts short-period motions for three of the events, while the H96 source model significantly overpredicts short-period motions for most events. The H96 model provides accurate predictions for the Mont Laurier (M 4.5) and Saguenay (M 5.8) events; it is the only model that matches the Saguenay observations.

At long periods (≥ 1 sec), all of the source models tend to overpredict the observed ground-motion amplitudes to some degree, at least for the ENA events. The overprediction is modest for the BC92, AB95, J97, and modified California (AB98-Ca) models; there is pronounced overprediction of motions for the Fea96, H96, and TAS97 models. These trends persist over the entire range of magnitudes.

Figure 5 summarizes the mean bias as a function of period, averaged first over just the ENA events then over all events. In computing the bias, the correlation of residuals

for a given earthquake has been accounted for, using the maximum likelihood scheme of Joyner and Boore (1993, 1994). From this figure, the key conclusions of our comparisons can be drawn. These conclusions are similar regardless of whether the non-ENA intraplate events are included. All source models, with the exception of the Boatwright and Choy (1992) model, tend to be conservative overall; in other words, the models generally overpredict the observed motions. The amount of the overprediction is relatively small (i.e., factor < 1.2) for the Atkinson and Boore (1995) relations, for periods ≤ 2 sec. The Joyner (1997a,b) model is also relatively accurate (within about 30%) for periods of 0.1 to 1 sec, although it overpredicts significantly at longer periods. There is significant overprediction (by more than 50%) at periods of 0.5 sec and greater for the Frankel *et al.* (1996) and Toro *et al.* (1997) relations, and large overprediction (by more than 100%) for the Haddon (1996) model. All relations tend to show a period dependence to the mean bias, with the bias growing increasingly negative as the period increases. When the non-ENA events are included, this trend is less pronounced. For the Atkinson and Boore (1995) relations, the inclusion of the additional data suggests that the ground-motion predictions are unbiased, to within a standard error of the mean, for all periods from 0.1 to 10 sec.

The pronounced overprediction of long-period amplitudes indicated in Figure 5 for most models (factors of 2 to 10) is highly significant with regards to the issue of source spectral shape. The data for periods from 2 to 10 sec come from earthquakes in the M 5.8 to 7.4 range (see Fig. 4). The source spectral levels for these events at very long periods (> 20 sec) are constrained by their seismic moments, as determined from teleseismic data. Under the single-corner-frequency Brune model, spectral amplitudes for events of $M < 7$ should converge to the long-period end of the spectrum (i.e., constant displacement spectrum) within the 5- to 10-sec period band; for the two-corner empirical model used by AB95, convergence with the moment end of the spectrum is pushed toward longer periods. The fact that observed spectral amplitudes in the 2- to 10-sec period range fall well below the required levels for the moment-end of the spectrum is strong evidence for a “sag” in the spectrum at intermediate periods, relative to the Brune model. This sag may be more pronounced than that incorporated into the AB95 relations, because these relations are also overpredicting the observations. These conclusions regarding the empirical evidence for an intermediate-period sag in the spectrum, relative to the Brune point-source model, echo those reached by Atkinson and Silva (1997) based on the much more extensive California ground-motion database.

The source model for the SSHAC (1996) ground-motion relations could not be evaluated directly. The SSHAC ground-motion predictions were derived from a workshop seeking to integrate the views of several ground-motion experts. The predictions take the form of ground-motion amplitudes for specific magnitude and distance values and have no particular underlying source model. However, the SSHAC

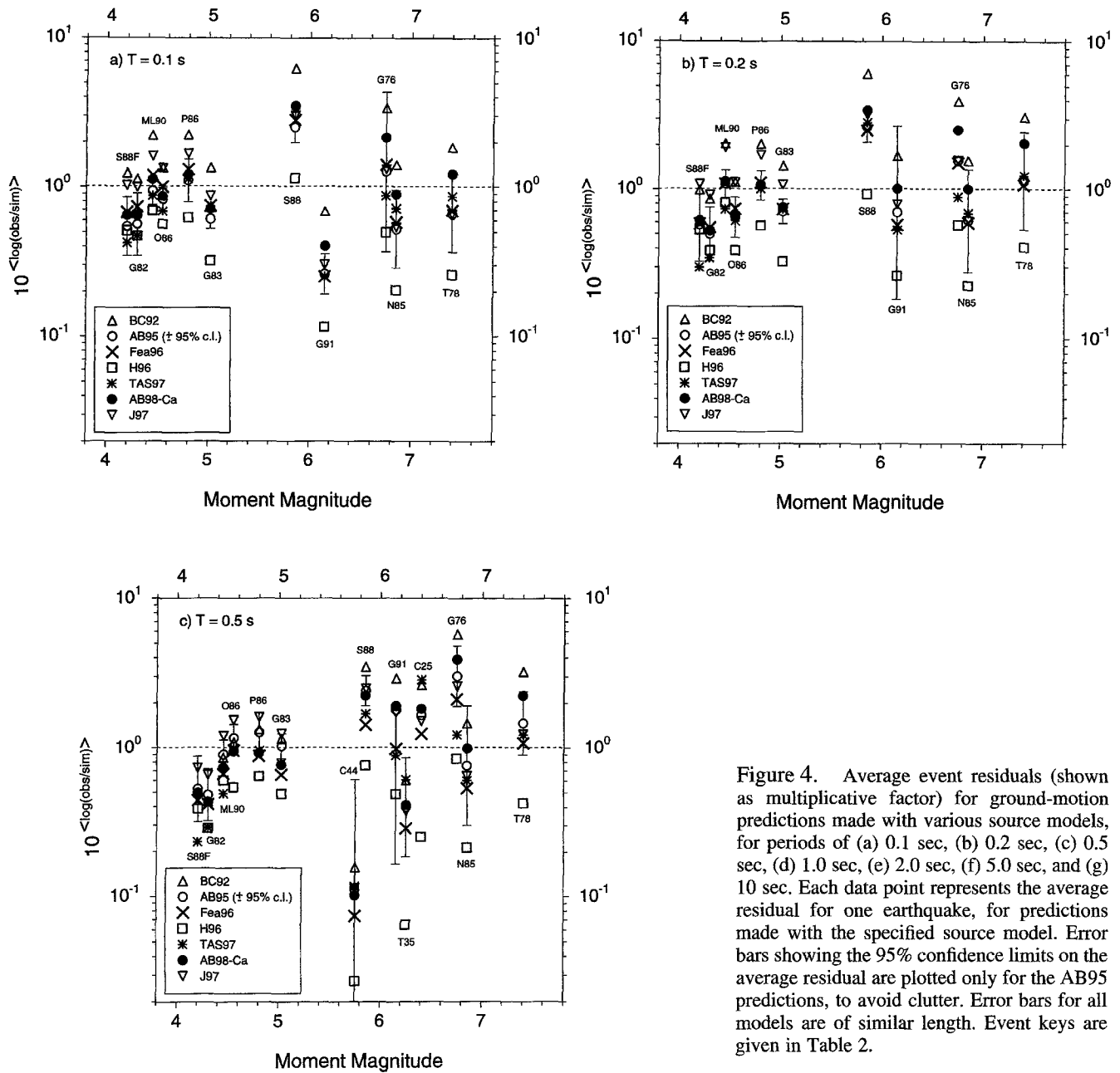


Figure 4. Average event residuals (shown as multiplicative factor) for ground-motion predictions made with various source models, for periods of (a) 0.1 sec, (b) 0.2 sec, (c) 0.5 sec, (d) 1.0 sec, (e) 2.0 sec, (f) 5.0 sec, and (g) 10 sec. Each data point represents the average residual for one earthquake, for predictions made with the specified source model. Error bars showing the 95% confidence limits on the average residual are plotted only for the AB95 predictions, to avoid clutter. Error bars for all models are of similar length. Event keys are given in Table 2.

ground-motion amplitudes are intermediate to those of Atkinson and Boore (1995) and EPRI (1993; also TAS97) [see Atkinson and Boore (1997)]. It follows that the SSHAC residuals plot about halfway between the AB95 and TAS97 residuals in Figures 4 and 5. Thus, the SSHAC model also significantly overpredicts motions at periods ≥ 1 sec.

Intensity Observations from Large Historical ENA Earthquakes

It is not feasible to use the historical intensity data directly in ground-motion modeling. Nevertheless, these data provide important constraints on earthquake source models, because the high-frequency source spectral level is closely correlated with felt area (Atkinson, 1993a). Figure 6 plots

the radius of the felt area of ENA earthquakes as a function of moment magnitude. The implied relationship between these quantities is shown for the source models of Boatwright and Choy (1992), Atkinson and Boore (1995), Haddon (1996), the Brune model as applied by Frankel *et al.* (1996), and the modified California model (AB98-Ca). The relationship between felt extent and moment magnitude for the Frankel *et al.* (1996) model is given by the theoretical relation of Frankel (1994), based on certain assumptions regarding scaling, attenuation, and the frequency of perceptible motions. For the other models, the felt area corresponding to each M value was computed based on its high-frequency source spectral level, using the empirical relationship between felt area and high-frequency spectral

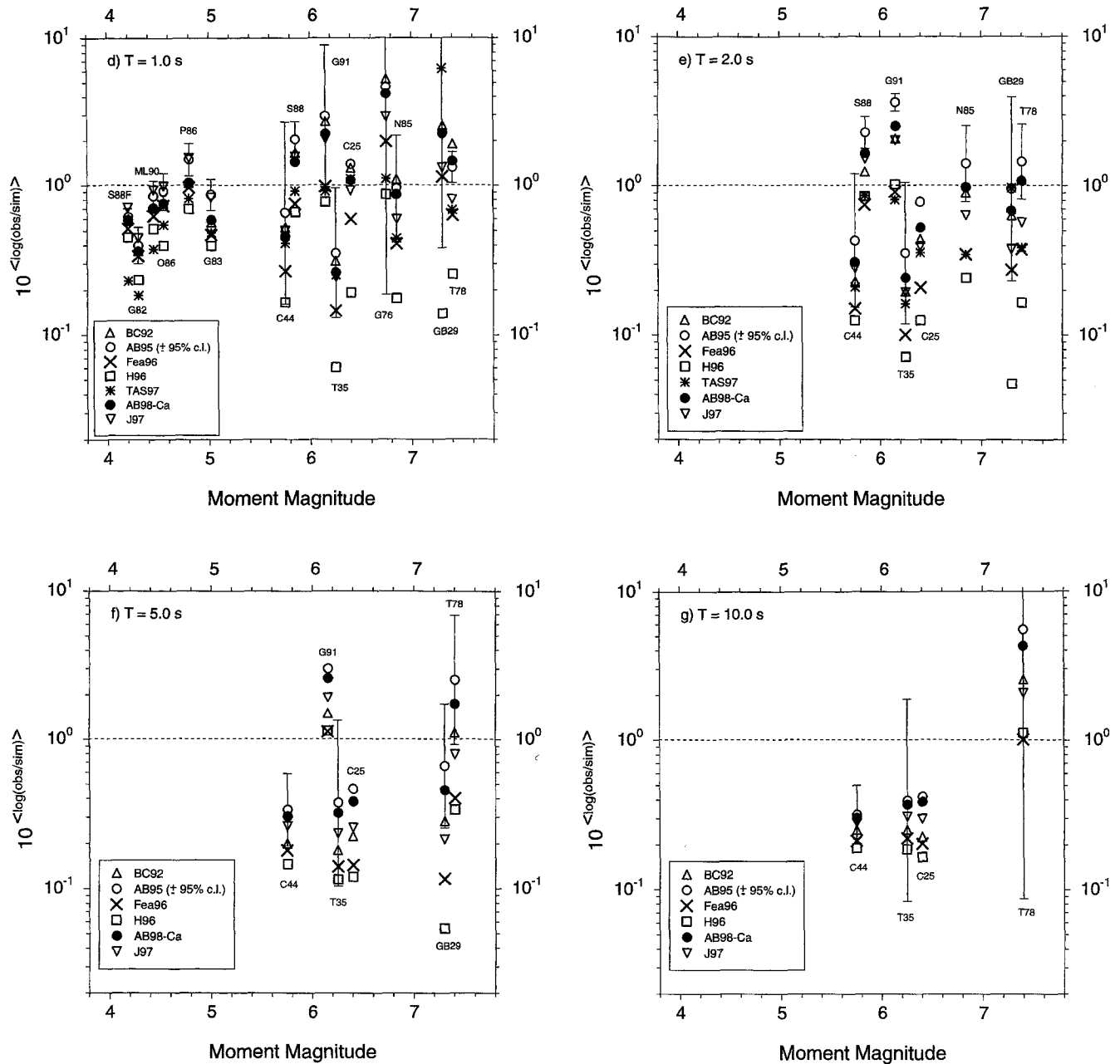


Figure 4. (continued)

level (e.g., Atkinson, 1993a). The source models used by Toro *et al.* (1997) and Joyner (1997a,b) were constrained to match the high-frequency levels of the Atkinson (1993a) source model, as used by Atkinson and Boore (1995). Therefore, it is not necessary to plot these relations separately: They would lie within the narrow range between the AB95 and Fea96 relations, depending on whether the theoretical (Frankel) or empirical (Atkinson) shape of this function is preferred. We conclude from Figure 6 that the high-frequency spectral amplitudes specified by the AB95, Fea96, TAS97, and J97 source models equal or exceed the levels inferred from the felt areas of most of the large ENA events, with the notable exception of the Saguenay earthquake.

These felt areas suggest that the high-frequency spectral levels implied by the BC92 model are somewhat low, whereas the high-frequency spectral levels of the H96 model are too high. The modified California model appears to be consistent with the felt areas; note that this implicitly includes ENA attenuation differences, through the use of an empirical ENA relation between high-frequency spectral level and felt area. This conclusion supports a similar finding by Hanks and Johnston (1992).

We note that the implied relationship between felt area and M for the Haddon source model is consistent with the MMI data for the Saguenay (and Mont Laurier) earthquakes; the AB95 and Fea96 models are not consistent with the Sag-

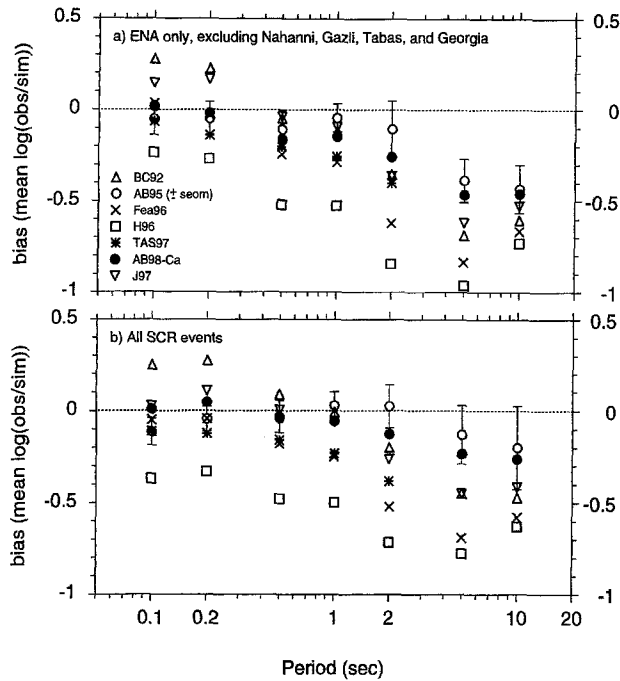


Figure 5. Mean bias evaluated over all events (maximum likelihood estimate), for each of the source models used to make ground-motion predictions. Error bars show the standard error of the mean bias, for the AB95 model; error bars for all models are of similar length. (a) Shows mean bias computed using just the ENA events. (b) Shows mean bias including data from ENA and other analogous regions (e.g., including Nahanni, Gazli, Tabas, and Georgia events).

uenay data. This points to the root of the problem: models that fit the Saguenay data—be it intensity data, strong-ground-motion data, regional seismographic data, or tele-seismic data—will not fit the rest of the data.

Long-Period Behavior of Source Spectrum (M_s - M relation)

The ENA database is particularly weak for long-period motions from large events. This aspect of the source spectrum is perhaps the most controversial and exhibits the largest discrepancies among proposed alternative models. It has been suggested that it may be possible to discriminate among the alternative models discussed in this article on the basis of the observed relationship between surface-wave magnitude (M_s) and moment magnitude (T. Hanks, personal comm., 1997). Indeed, such relationships are frequently exploited in the development or testing of spectral scaling models and have been used in previous studies to support the concept of a “spectral sag” (Gusev, 1983; Boore, 1986). Specifically, a prominent sag in the long-period spectrum implies a lesser value of M_s , for a given M , relative to the Brune model.

In Figure 7, we plot the M_s - M relationship implied by

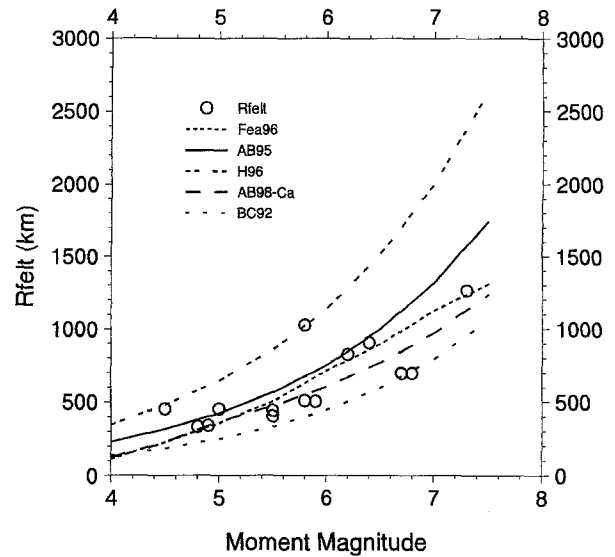


Figure 6. Comparison of the felt area implied by the evaluated source models (lines), in relation to felt areas of historical ENA earthquakes (symbols). The lines corresponding to the TAS97 and J97 models (not shown) would plot in the range between the AB95 and Fea96 lines.

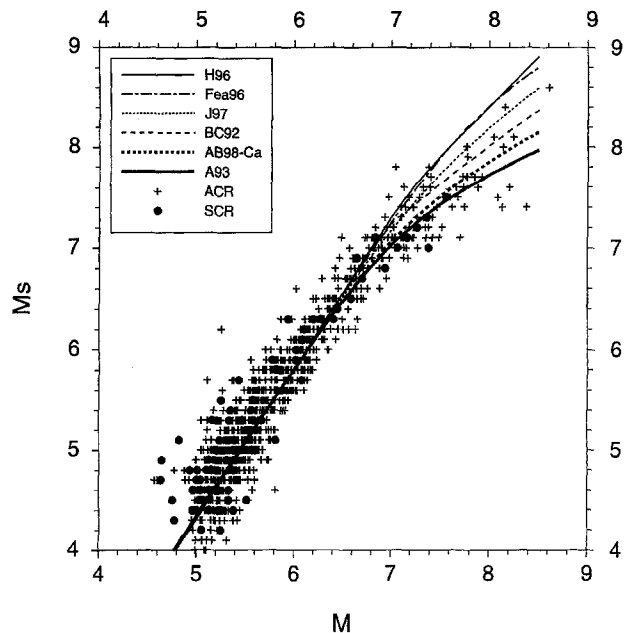


Figure 7. Relationship between surface-wave magnitude and moment magnitude. Lines show relations implied by the source spectral models. Symbols show database of Triep and Sykes (1996) for active continental regions (ACR) and stable continental regions (SCR).

each of the source spectral models, in comparison to data from stable continental regions (SRC) and active continental regions (ACR) (data compiled by Triep and Sykes, 1996). The M_s - M scaling implied by each of the source spectral models was determined as follows. First, from the definition of M_s , it follows that M_s scales directly with the log of the source spectrum at a period of 20 sec; this establishes the shape of the curve (i.e., magnitude scaling) for each of the models. To constrain the level of the curves, we require that each curve predict $M_s = 6$ for $M = 6$ (i.e., all curves go through this point); this requirement forces the result that all models agree in the magnitude range where the data are most abundant.

The comparison of the magnitude scaling relations to data adds limited support for the empirical two-corner models, A93 and AB98-Ca. The AB98-Ca model appears to provide the best match to the data. All other source models appear, on average, to overestimate M_s for $M > 7$. The overprediction is pronounced for the Fea96 and H96 models. However, it is acknowledged that the data are sparse and highly variable for $M > 7$, and the differences between the models are relatively small for $M < 7.4$.

Conclusions

The ENA ground-motion database, though sparse, is sufficient to discriminate among alternative models of the earthquake source spectrum that have been proposed for use in the development of regional ground-motion relations. Our main conclusions can be drawn from Figure 5. We caution that in interpreting Figure 5, it is important to bear the magnitude distribution of the underlying events in mind (Fig. 1).

ENA Data Only (Fig. 5a)

For the existing ENA database, comprised largely of moderate events, all of the earthquake source models that we evaluated overpredict observed ENA motions on rock sites at long periods (>2 sec). At short-to-intermediate periods (0.1 to 2 sec), the Atkinson and Boore (1995) model is the least biased. The AB95 relations tend to overpredict the observed data by about a factor of 1.2 or less; the residuals for the AB95 model fall within the standard error of an unbiased prediction. The tendency toward overprediction suggests that the sag in spectral amplitudes relative to the Brune model may be more pronounced in the data than in the underlying source model used by AB95.

The Frankel *et al.* (1996) model significantly overpredicts the motions for periods of 0.5 sec and greater, and the Haddon (1996) model overpredicts the motions by more than a factor of 2 on average for all periods. The Boatwright and Choy (1992) source model underpredicts short-period amplitudes but overpredicts intermediate- to long-period amplitudes. The Joyner (1997) source model has no significant bias in the period range from 0.1 to 1 sec but significantly overpredicts motions at periods of 2 sec and greater.

ENA and Other Mid-Plate Data (Fig. 5b)

The addition of several large events from other mid-plate regions significantly improves the magnitude–distance distribution of the database at large magnitudes and close distances (see Fig. 1). The expanded database strongly supports the AB95 ground-motion model: The residuals for the AB95 model are within the standard error of an unbiased prediction, for all periods from 0.1 to 10 sec. The modified California model, AB98-Ca, matches the database equally well. The Joyner (1997a,b) model provides an unbiased prediction for periods from 0.1 to 1 sec but overpredicts longer-period motions. All other models are in significant disagreement with the empirical database over most of the 0.1- to 10-sec period band.

The inclusion of non-ENA data does not significantly change the residuals, except for periods of 5 and 10 sec. These residuals are very uncertain, however, because they are based on very few data: Neither Nahanni nor Gazli have data at these periods. We infer that the classification of the Nahanni event is not a significant issue in judging the residuals.

We conclude that most recent ENA ground-motion relations overpredict observed ground-motion amplitudes by more than 40% on average, for periods ≥ 0.5 sec. Specifically, this assessment includes the relations of EPRI (1993), SSHAC (1995), Frankel *et al.* (1996), and Toro *et al.* (1997). The Atkinson and Boore (1995, 1997) ground-motion relations are in satisfactory agreement (within 20%) with the existing ENA ground-motion database, except at periods ≥ 5 sec (for which they are conservative). This agreement is not surprising, because the AB95 relations used the empirical database more directly in the development of the relations than did the other ground-motion relations. However, there is some independence in the comparisons: the digitized data from the four historical ENA earthquakes of $M > 5.5$ have only recently been added to the database, as have the data from large events in other mid-plate regions; thus 7 of the 15 events are “new,” in the sense that they were not used in our 1995 study. The Joyner (1997) source model would appear to offer a compromise between the Brune source model, upon which the EPRI, Frankel *et al.*, and Toro *et al.* relations were based, and the empirical source model of Atkinson, upon which the Atkinson and Boore relations were based.

Application of California Ground-Motion Relations to ENA

The empirical California source model (AB98-Ca) is remarkably similar to the empirical ENA source model (AB95), when adjustments are made to account for regional differences in crustal velocity structure and near-surface attenuation. For this reason, the modified California source model does a credible job of predicting the observed ENA amplitudes, when used with ENA attenuation parameters.

There is some period dependence to the bias, which could be attributed either to regional differences in source properties or to inaccurate estimation of the effects of differences in the regional crustal velocity structure. The implication is that California ground-motion relations may be applicable to ENA if appropriate corrections for regional differences in crustal properties can be made. This supports the conclusions of Hanks and Johnston (1992) that apparent differences in the source radiation between the two regions may not be significant.

There is an important engineering application of this conclusion. Empirical California ground-motion relations, suitably modified for the eastern crustal velocity gradient and attenuation, may be used to predict ground motion for future large earthquakes in ENA. This is an attractive approach because the empirical ground-motion relations for California are firmly based in data for much of the magnitude–distance range of interest and also contain empirical representations of a number of complex effects, including finite-fault effects and nonlinearity.

We must emphasize the phrase *suitably modified*. The corrections made for crustal effects are large. The use of California relations without these corrections would result in large errors in prediction. Because we believe this to be an important application, we have tabulated the required correction factors, which depend on period and distance but are independent of magnitude. The correction factors are the *inverse* of the product of four processes:

- multiplicative constant C for source spectrum (from equation 1) is higher in California than in ENA, by the ratio $(\rho\beta^3)_{Ca}/(\rho\beta^3)_{ENA}$;
- amplification through the generic crustal profile for California rock (Boore and Joyner, 1997); this amplifies California motions relative to ENA motions;
- high-frequency diminution attributable to the California kappa operator, with assumed California $\kappa = 0.04$ (Anderson and Hough, 1984); this reduces high-frequency motions in California relative to ENA motions; and
- effects of regional differences in Q , modeled by the ratio of anelastic attenuation in California (from Atkinson and Silva, 1997) to that in ENA (from Atkinson and Boore, 1995); this results in more rapid fall-off of California motions with distance.

It is implicitly assumed that (1) regional differences in geometric spreading and ground-motion duration are not significant in the distance range of interest and that (2) the ratio of regional anelastic attenuation factors is a reasonable approximation of the differences in the shapes of the attenuation curves. We limit the factors to distances within 100 km of the source, in order to stay within the range of validity of the California ground-motion relations.

Table 6 provides the multiplicative scaling factors that should be applied to ground motions computed from California ground-motion relations, in order to predict the equiv-

Table 6
Ratio of Eastern/California Ground-Motion Amplitudes

HypoR (km)	Period (sec)							
	0.08	0.16	0.31	0.63	1.25	2.50	5.00	10.00
5	1.192	0.638	0.503	0.500	0.543	0.571	0.633	0.685
10	1.236	0.657	0.515	0.509	0.551	0.577	0.638	0.690
15	1.282	0.677	0.527	0.519	0.559	0.584	0.644	0.694
20	1.329	0.698	0.540	0.529	0.567	0.591	0.649	0.699
30	1.429	0.740	0.566	0.549	0.584	0.604	0.661	0.708
50	1.653	0.834	0.623	0.592	0.619	0.632	0.684	0.727
70	1.911	0.939	0.686	0.638	0.657	0.661	0.708	0.747
100	2.376	1.122	0.791	0.715	0.717	0.708	0.746	0.777

Note: These multiplicative factors may also be obtained by the following equation:

$$\text{Ratio ENA/California} = c_1 + c_2 R + R^2$$

Period	Ratio ENA/California = $c_1 + c_2 R + R^2$							
	0.08	0.16	0.31	0.63	1.25	2.50	5.00	10.00
c_1	1.155	0.621	0.491	0.491	0.535	0.565	0.627	0.681
c_2	0.00772	0.00350	0.00228	0.00182	0.00155	0.00127	0.00108	8.96E-4
c_3	4.48E-05	1.50E-5	7.24E-6	4.25E-6	2.69E-6	1.63E-6	1.03E-6	6.35E-7

Values for other periods may be obtained by interpolation.

alent ground-motion amplitudes for events of the same moment magnitude, occurring in ENA. Values for intermediate distances may be obtained by interpolation or by using the equation provided in the table. These factors implicitly include the effects of higher shear-wave velocity for generic eastern rock sites, as compared to generic California rock sites. Therefore, if the factors are applied to empirical relations for California rock sites, they will provide motions for the hard-rock sites that are typical for ENA.

We illustrate this technique in Figure 8, which compares the empirical California ground-motion relations of Abrahamson and Silva (1997) for generic California soft-rock sites ($\beta \approx 600$ m/sec in the top 30 m), modified by applying the multiplicative factors of Table 6, to the ENA ground-motion relations of AB95 and TAS97. At short periods, the modified California relations closely follow the ENA relations for **M** 5. At **M** 7, the modified California ground-motion relations suggest a saturation of near-source amplitudes, relative to the constant-stress high-frequency scaling that is inherent in the ENA models. This is consistent with the findings of Atkinson and Silva (1997) (e.g., apparent decrease in Brune stress drop with increasing magnitude) and may be an indication of pervasive nonlinearity in the California short-period amplitudes at large magnitudes and close distances. This nonlinearity would not be present in the ENA relations, because the shear-wave velocity of generic ENA rock sites is much higher. We infer that use of the modified California relations in ENA may underestimate near-source short-period ground motions from large events, on rock sites. This inference may appear inconsistent with our conclusion that the modified empirical California source model, which has embedded in it any nonlinearity in the California soft-rock data, is successful at predicting the observed ENA ground-motion database for rock sites. However, large-mag-

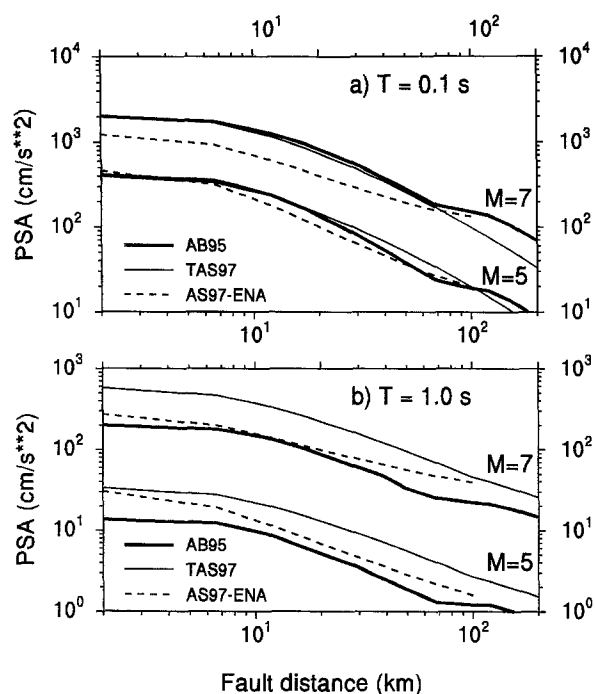


Figure 8. Comparison of eastern ground-motion relations of Atkinson and Boore (1995) (AB95) and Toro *et al.* (1997) (TAS97), for rock sites, to corresponding relations implied by modification of empirical California ground-motion relations (as discussed in text) of Abrahamson and Silva (1997) (AS97). Comparison is plotted for response spectra at periods of (a) 0.1 sec and (b) 1.0 sec.

nitude data at near-source distances are available only for the Nahanni, Gazli, and Tabas events. The AB98-Ca model shows a slight tendency to underpredict motions from the Gazli and Tabas events at short periods (consistent with our inference from Fig. 8), but the data are too sparse to be conclusive at this point. We do not view the potential underestimation of near-source short-period rock motions, from large events, as a serious limitation of this technique for most seismic hazard applications; however, the reader should be aware of this caveat.

At longer periods (1 sec), for which nonlinear behavior is not expected (Abrahamson and Silva, 1997), the modified California ground-motion relations are remarkably consistent with the AB95 relations, particularly for large events. The TAS97 relations predict large 1-sec amplitudes for M 7 events, which are difficult to reconcile with California empirical relations.

The factors of Table 6 are also applicable to any other surficial soil condition represented by the empirical California ground-motion relations. For example, these factors can be applied to obtain ENA motions on soil from California ground-motion relations for soil sites, provided the shear-wave velocity profiles of the soil sites are comparable. By application of the factors in Table 6, then, any empirical

ground-motion relation for California can be adjusted to provide predictions for comparable events in ENA.

Acknowledgments

Financial support for this work was provided by the Natural Sciences and Engineering Research Council of Canada, the U.S. Nuclear Regulatory Commission, and the National Earthquake Hazards Reduction Program. We are grateful to Tom Hanks, Arch Johnston, Bill Joyner, and Christine Powell for their constructive reviews.

References

- Abrahamson, N. and K. Shedlock (1997). Overview (of Special Ground Motion Issue), *Seism. Res. Lett.* **68**, 9–23.
- Abrahamson, N. and W. Silva (1997). Empirical response spectral attenuation relations for shallow crustal earthquakes, *Seism. Res. Lett.* **68**, 94–127.
- Anderson, J. and S. Hough (1984). A model for the shape of the Fourier amplitude spectrum of acceleration at high frequencies, *Bull. Seism. Soc. Am.* **74**, 1969–1993.
- Atkinson, G. (1993a). Source spectra for earthquakes in eastern North America, *Bull. Seism. Soc. Am.* **83**, 1778–1798.
- Atkinson, G. (1993b). Notes on ground motion parameters for eastern North America: duration and H/V ratio, *Bull. Seism. Soc. Am.* **83**, 587–596.
- Atkinson, G. (1995). Optimal choice of magnitude scales for seismic hazard analysis, *Seism. Res. Lett.* **66**, 51–55.
- Atkinson, G. and D. Boore (1995). New ground motion relations for eastern North America, *Bull. Seism. Soc. Am.* **85**, 17–30.
- Atkinson, G. and D. Boore (1997). Some comparisons of recent ground motion relations, *Seism. Res. Lett.* **68**, 24–40.
- Atkinson, G. and S. Chen (1997). Regional seismograms from historical earthquakes in southeastern Canada, *Seism. Res. Lett.* **68**, 797–807.
- Atkinson, G. and T. Hanks (1995). A high-frequency magnitude scale, *Bull. Seism. Soc. Am.* **85**, 825–833.
- Atkinson, G. and W. Silva (1997). Empirical source spectra for California earthquakes, *Bull. Seism. Soc. Am.* **87**, 97–113.
- Atkinson, G. and P. Somerville (1994). Calibration of time history simulation methods, *Bull. Seism. Soc. Am.* **84**, 400–414.
- Beresnev, I. and G. Atkinson (1997). Shear wave velocity survey of seismographic sites in eastern Canada: calibration of empirical regression method of estimating site response, *Seism. Res. Lett.* **68**, 981–987.
- Boatwright, J. (1994). Regional propagation characteristics and source parameters of earthquakes in eastern North America, *Bull. Seism. Soc. Am.* **84**, 1–15.
- Boatwright, J. and G. Choy (1992). Acceleration source spectra anticipated for large earthquakes in Northeastern North America, *Bull. Seism. Soc. Am.* **82**, 660–682.
- Bollinger, G., M. Chapman, and M. Sibol (1993). A comparison of earthquake damage areas as a function of magnitude across the United States, *Bull. Seism. Soc. Am.* **83**, 1064–1080.
- Boore, D. (1983). Stochastic simulation of high-frequency ground motions based on seismological models of the radiated spectra, *Bull. Seism. Soc. Am.* **73**, 1865–1894.
- Boore, D. (1986). Short-period P- and S-wave radiation from large earthquakes: implications for spectral scaling relations, *Bull. Seism. Soc. Am.* **76**, 43–64.
- Boore, D. (1996). SMSIM—Fortran program for simulating ground motions from earthquakes: Version 1.0 *U.S. Geol. Surv. Open-File Rept.* 96-80-A.
- Boore, D. and G. Atkinson (1987). Stochastic prediction of ground motion and spectral response parameters at hard-rock sites in eastern North America, *Bull. Seism. Soc. Am.* **77**, 440–467.
- Boore, D. and G. Atkinson (1989). Spectral scaling of the 1985–1988 Na-

- hanni, Northwest Territories, earthquakes, *Bull. Seism. Soc. Am.* **79**, 1736–1761.
- Boore, D. and W. Joyner (1997). Site amplifications for generic rock sites, *Bull. Seism. Soc. Am.* **87**, 327–341.
- Brune, J. (1970). Tectonic stress and the spectra of seismic shear waves from earthquakes, *J. Geophys. Res.* **75**, 4997–5009.
- Brune, J. (1971). Correction, *J. Geophys. Res.* **76**, 5002.
- EPRI (1993). *Guidelines for Determining Design Basis Ground Motions. Early Site Permit Demonstration Program*, Vol. 1, RP3302, Electric Power Research Institute, Palo Alto, California.
- Frankel, A. (1994). Implications of felt area-magnitude relations for earthquake scaling and the average frequency of perceptible ground motion, *Bull. Seism. Soc. Am.* **84**, 462–465.
- Frankel, A., C. Mueller, T. Barnhard, D. Perkins, E. Leyendecker, N. Dickman, S. Hanson, and M. Hopper (1996). National seismic hazard maps, June 1996, *U.S. Geol. Surv. Open-File Rept.* 96-532.
- Gusev, A. (1983). Descriptive statistical model of earthquake source radiation and its application to an estimate of short-period strong motion, *Geophys. J. R. Astr. Soc.* **74**, 787–808.
- Haddon, R. (1996). Earthquake source spectra in eastern North America, *Bull. Seism. Soc. Am.* **86**, 1300–1313.
- Haddon, R. (1997). Reply to Comment on “Earthquake source spectra in eastern North America” by Atkinson, Boore, and Boatwright, *Bull. Seism. Soc. Am.* **87**, 1703–1708.
- Hanks, T. and A. Johnston (1992). Common features of the excitation and propagation of strong ground motion for North American earthquakes, *Bull. Seism. Soc. Am.* **82**, 1–23.
- Hanks, T. and H. Kanamori (1979). A moment magnitude scale, *J. Geophys. Res.* **84**, 2348–2350.
- Hanks, T. and R. McGuire (1981). The character of high-frequency strong ground motion, *Bull. Seism. Soc. Am.* **71**, 2071–2095.
- Johnston, A. (1996). Seismic moment assessment of earthquakes in stable continental regions, *Geophys. J. Intl.* **124**, 381–414 (Part I); **125**, 639–678 (Part II); **126**, 314–344 (Part III).
- Joyner, W. (1997a). Ground motion estimates for the northeastern U.S. or southeastern Canada, in *Recommendations for Probabilistic Seismic Hazard Analysis: Guidance on Uncertainty and Use of Experts*, Senior Seismic Hazard Analysis Committee (R. Budnitz, G. Apostolakis, D. Boore, L. Cluff, K. Coppersmith, A. Cornell, and P. Morris), U.S. Nuclear Reg. Comm. Rept. NUREG/CR-6372, Washington, D.C.
- Joyner, W. (1997b). Errata to equations of 1997a, personal communication.
- Joyner, W. and D. Boore (1993). Methods for regression analysis of strong-motion data, *Bull. Seism. Soc. Am.* **83**, 469–487.
- Joyner, W. and D. Boore (1994). Errata, *Bull. Seism. Soc. Am.* **84**, 955.
- Ou, G. and R. Herrmann (1990). A statistical model for peak ground motion from local to regional distances, *Bull. Seism. Soc. Am.* **80**, 1397–1417.
- SSHAC (1996). *Recommendations for Probabilistic Seismic Hazard Analysis: Guidance on Uncertainty and Use of Experts*, Senior Seismic Hazard Analysis Committee (R. Budnitz, G. Apostolakis, D. Boore, L. Cluff, K. Coppersmith, A. Cornell, and P. Morris), Available as NUREG/CR-6372, U.S. Nuclear Reg. Comm., Washington, D.C.
- Toro, G. and R. McGuire (1987). An investigation into earthquake ground motion characteristics in eastern North America, *Bull. Seism. Soc. Am.* **77**, 468–489.
- Toro, G., N. Abrahamson, and J. Schneider (1997). Model of strong ground motion in eastern and central North America: best estimates and uncertainties, *Seism. Res. Lett.* **68**, 41–57.
- Triep, E. and L. Sykes (1996). Catalog of shallow intracontinental earthquakes. <http://www.ldeo.columbia.edu/seismology/triep/intra.expl.html> (also submitted to *J. Geophys. Res.*, 1996).
- Wetmiller, R., R. Horner, H. Hasegawa, R. North, M. Lamontagne, D. Weichert, and S. Evans (1988). An analysis of the 1985 Nahanni earthquakes, *Bull. Seism. Soc. Am.* **78**, 590–616.

Department of Earth Sciences
 Carleton University
 1125 Colonel By Drive
 Ottawa, Ontario K1S 5B6
 (G.M.A.)

U.S. Geological Survey
 345 Middlefield Road
 Menlo Park, California 94025
 (D.M.B.)

Manuscript received 1 October 1997.